Extensions of the Common-Reflection-Surface Stack Considering the Surface Topography and the Near-Surface Velocity Gradient

Zeno Heilmann, Geophysical Institute, University of Karlsruhe

Summary

Two years ago a generalized 2-D *zero-offset* (ZO) *Common-Reflection-Surface* (CRS) stack formula was presented by Chira et al. (2001). This traveltime equation enables to stack seismic data, considering the average dip and curvature of the measurement surface within the stacking aperture and the near-surface velocity gradient at the emergence point of the respective ZO ray. Nevertheless, the CRS stack procedure has remained purely data-driven, i.e., independent of the a priori unknown macro velocity model. Besides the average dip and curvature of the measurement surface, only the near-surface velocity and its gradient in the vicinity of the considered coincident source and receiver points are required. As in case of a planar measurement surface, three wavefield attributes are determined that provide important informations about the investigated subsurface structure. These can be applied in a number of kinematic and dynamic modeling, inversion, and stacking problems. In this abstract, a modified formulation of this 2-D CRS traveltime formula is presented. The new formula is better suited for the practical application, because the previously used local coordinate system of every considered ZO location is substituted by a global coordinate system. By this means, time consuming transformations of the input data can be avoided and an extension of the existing 2-D ZO CRS stack software, designed for planar measurement surfaces, only, is simplified. In addition, a redatuming procedure is presented that relates the obtained results to a virtual planar measurement surface with constant near-surface velocity. This step is very important to simplify subsequent interpretation and further processing, because otherwise the resulting stack and attribute sections would be strongly influenced by the top-surface topography and its potentially inhomogeneous top-layer.

Introduction

As is generally known, the goal of stacking is to reduce the amount of data and to enhance its signal-to-noise ratio by summing up correlated events in the multi-coverage data. As result, a well interpretable time domain image of the subsurface is achieved and important attributes like, e.g., the *normal moveout* (NMO) velocity are determined. Today, various kinds of stacking operators are in use. In general, a 2-D ZO stacking operator, as discussed in this abstract, describes a surface or curve in the midpoint-offset-traveltime space that approximates an actual reflection response measured in the vicinity of the emergence point of the considered ZO ray. This ray is associated with a technically not applicable experiment where source and receiver are coincident. The summation result along the ZO stacking operator is assigned to the respective point in the zero-offset plane of the midpoint-offset-traveltime data volume. Doing this for all points of this so-called *ZO section* yields the stacked ZO section, which is very valuable for interpretation due to its specific geometry and high signal-to-noise ratio. Well-known conventional ZO stacking methods are the *common-midpoint* (CMP) stack and the *normal-moveout/dip-moveout* (NMO/DMO) stack process. Within the last years, the *Common-Reflection-Surface* (CRS) stack has been established as a promising alternative to the seismic reflection imaging methods used so far. Originally designed to generate a 2-D ZO stack section (Höcht, 1998; Müller, 1999; Mann, 2002), the CRS stack was successfully extended to 3-D (Höcht, 2002) and for finite-offset (FO) (Zhang et al., 2001; Bergler, 2001). Conventional stacking methods, like, e.g., the CMP stack, are based on very simple velocity-model assumptions and use one-parametric traveltime formulas that are applied to common-midpoint data only. The CRS stack makes use of the full multi-coverage seismic-reflection data and provides additional traveltime parameters. These parameters are very useful for the extraction of further attributes of the seismic medium or to obtain a subsurface-velocity model (Duveneck, 2003). Another important feature of the CRS stack method is that the a priori unknown macro-velocity model is not required. For this reason, this method belongs to the macro-model independent methods, which also include the Polystack method (de Bazelaire, 1988; de Bazelaire and Viallix, 1994) and the Multifocusing method (Gelchinsky et al., 1997). For a detailed discussion of various aspects of macro-model independent reflection imaging methods, I refer to Hubral (1999).

Practical experiences have shown that these new methods are particularly successful for seismic land data. However, land data suffer in many cases from complex near-surface conditions like laterally changing near-surface velocities and undulating topography. That is why the existing CRS method was generalized to handle such situations (Chira et al., 2001). Until then, all discussions and derivations in this regard had involved a planar measurement surface, even though the assumption of a planar measurement surface is, by no means, a requirement for the validity of the *surface-to-surface propagator matrix* formalism (Bortfeld, 1989), which is the basis of the derivation of the CRS traveltime formulas. Finally, it has to be mentioned that an extension of the Multifocusing method, designed to include the topographic features of the measurement surface, has also been proposed in Gurevich et al. (2001), and that an alternative CRS stack approach, considering even rough topography, was recently presented by Zhang et al. (2002).

A general 2-D CRS stacking operator in global coordinates

In order to approximate the reflection response of an unknown reflector segment in depth, the CRS stack uses a second order Taylor expansion of the traveltime moveout. This traveltime moveout is related to the corresponding ZO ray, defined by its coincident source and receiver location $X_0(x_0,z_0)$ and its ZO traveltime t_0. Consequently, every point in the ZO section is related to one ZO ray, called the *central ray*, and one CRS stacking operator.
If one introduces midpoint m and half-offset h coordinates instead of the source and receiver locations x_S and x_G, according to the relations

$$m = \frac{x_S + x_G}{2} \quad \text{and} \quad h = \frac{x_G - x_S}{2} \,, \tag{1}$$

one obtains a parabolic traveltime formula that reads

$$t_{par} = t_0 + \sigma_1\, m + \sigma_2\, m^2 + \sigma_3\, h^2 \,, \tag{2}$$

where $\sigma_1, \sigma_2, \sigma_3$ are the Taylor expansion coefficients. Squaring this equation and retaining only the terms up to the second order in m and h leads to the corresponding hyperbolic representation

$$t_{hyp}^2 = (t_0 + \sigma_1\, m)^2 + 2 t_0 (\sigma_2\, m^2 + \sigma_3\, h^2) \,. \tag{3}$$

It has to be mentioned that x_S, x_G, m, and h are 1D coordinates, measured along the tangent to the measurement surface in X_0, in a local coordinate system with its origin in X_0. For the sake of simplicity, only the hyperbolic formula is considered in the following, as it is more successful in practice (see, e.g., Höcht, 1998; Müller, 1999).

Using paraxial ray theory, Chira et al. substituted the three Taylor coefficients by physical properties of the measurement surface and its subsurface. All used properties are related to the considered central ray and can be measured in X_0 and its vicinity. The derivation requires the following assumptions:

1. Within the stacking aperture, the measurement surface is representable by a parabola with origin in X_0.
2. There are only first order near-surface velocity variations.

The obtained traveltime equation reads

$$\begin{aligned} t_{hyp}^2 = & \left(t_0 + 2\,\frac{\sin\beta_0}{v_0}\, m \right)^2 \\ & + \frac{2\,t_0}{v_0} \left(K_N\, \cos^2\beta_0 - K_0\, \cos\beta_0 - v_0\, E_0 \right) m^2 \\ & + \frac{2\,t_0}{v_0} \left(K_{NIP}\, \cos^2\beta_0 - K_0\, \cos\beta_0 - v_0\, E_0 \right) h^2 \,, \end{aligned} \tag{4}$$

with

$$E_0 = -\frac{\sin\beta_0}{v_0^2} \Big[(1+\cos^2\beta_0)(\partial_x v)_0 + \cos\beta_0 \sin\beta_0\, (\partial_z v)_0 \Big] \,. \tag{5}$$

Here, $(\partial_{x_0} v)_0$ and $(\partial_{z_0} v)_0$ denote the 2D in-plane components of the medium-velocity gradient (∇v) at X_0. The searched for *wavefield attributes* are β_0, i.e., the emergence angle of the central ray (see Figure (2)), and K_N, K_{NIP}, two wavefront curvatures related to hypothetical experiments firstly introduced by Hubral (1983). The parameters v_0, the near-surface velocity, and K_0, the surface curvature, are assumed to be known a priori. The inhomogeneity factor E_0 depends, besides v_0 and β_0, on the near-surface velocity gradient $(\nabla v)_0$ which is also assumed to be a priori known.

As mentioned before, this traveltime formula assumes a local Cartesian coordinate system with its x-axis tangent to the measurement surface in X_0. This is the coordinate system where, according to Equation (1), half-offset h and midpoint m are defined. However, for the practical application, it is very inconvenient to transfer the globally measured (e.g., by GPS) source and receiver coordinates into the specific local coordinate system of every X_0 location that is to be considered. To solve this problem, I have used a coordinate transformation that transfers the different local coordinate systems to one global coordinate system with its x-axis parallel to the horizontal and its z-axis parallel to the depth direction. According to Figure (1) this transformation reads

$$h = \frac{1}{\cos\alpha_0}\, h_g \quad \text{and} \quad m = \frac{1}{\cos\alpha_0}\, (m_g - x_0) \,, \tag{6}$$

where m_g, h_g are the new offset and midpoint coordinates measured in the global coordinate system, x_0 is the global x-coordinate of point X_0, and α_0 is the dip of the local coordinate system in X_0 with respect to the horizontal.

If one applies this coordinate transformation to Equation (4), one gets a new traveltime equation which depends now explicitly on the dip angle α_0 of the measurement surface in X_0:

$$\begin{aligned} t_{hyp}^2 = & \left(t_0 + 2\,\frac{\sin\beta_0}{v_0 \cos\alpha_0}\, (m_g - x_0) \right)^2 \\ & + \frac{2\,t_0}{v_0 \cos^2\alpha_0} \left(K_N\, \cos^2\beta_0 - K_0\, \cos\beta_0 - v_0\, E_0 \right) (m_g - x_0)^2 \\ & + \frac{2\,t_0}{v_0 \cos^2\alpha_0} \left(K_{NIP}\, \cos^2\beta_0 - K_0\, \cos\beta_0 - v_0\, E_0 \right) h_g^2 \,. \end{aligned} \tag{7}$$

Please note that no additional parameter was introduced, as the surface dip is implicitly included in Equation (4), too.

To transpose the velocity gradient from local to global coordinates one has to perform a rotation of the coordinate system by the dip-angle α_0, which leads to the relation

$$(\nabla v)_0 = \begin{pmatrix} \cos\alpha_0 & \sin\alpha_0 \\ -\sin\alpha_0 & \cos\alpha_0 \end{pmatrix} (\nabla v)_0^g. \tag{8}$$

Inserting this relation into Equation (5), one obtains the inhomogeneity factor E_0 in global coordinates:

$$\begin{aligned} E_0 = -\frac{\sin\beta_0}{v_0^2} \Bigg[& (1+\cos^2\beta_0) \left(\cos\alpha_0 \left(\frac{\partial v}{\partial x_g}\right)_0 + \sin\alpha_0 \left(\frac{\partial v}{\partial z_g}\right)_0 \right) \\ & + \cos\beta_0 \sin\beta_0 \left(-\sin\alpha_0 \left(\frac{\partial v}{\partial x_g}\right)_0 + \cos\alpha_0 \left(\frac{\partial v}{\partial z_g}\right)_0 \right) \Bigg] \,. \end{aligned} \tag{9}$$

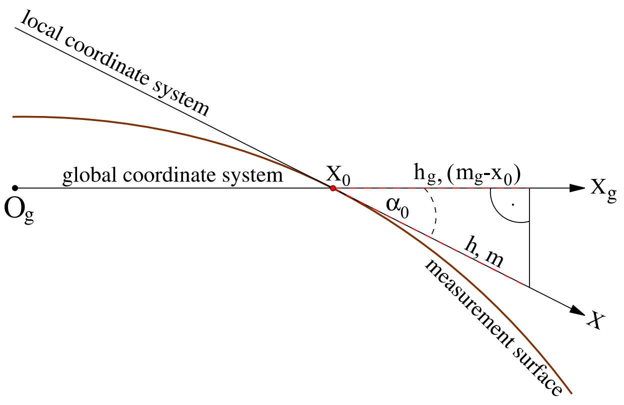

Figure 1: *The transformation of the local 1D midpoint and half-offset coordinates h and m to the respective global 1D coordinates h_g and m_g.*

Redatuming

As mentioned before, the final goal of the CRS stack is to provide a stacked ZO section and different wavefield attribute sections, which are the β_0 section, the K_N section, the K_{NIP} section, and the v_{NMO} section. It is evident that these sections should not depend on the characteristics of the measurement surface and of the potentially inhomogeneous top-layer. If the acquisition topography and the near-surface medium meet the required conditions, then Equations (4) and (7) are valid to determine the surface and near-surface medium independent wavefield attributes K_N and K_{NIP}. However, the obtained values of the NMO velocity are strongly influenced by the measurement surface and its top-layer and the take-off angle β_0 is still defined in the local coordinate system. In addition, all traces of the obtained sections are related to a floating datum. According to Figure (2), β_0 can easily be transferred to the surface-dip independent take-off angle β_0^g, which is measured with respect to the vertical. This transformation reads

$$\beta_0^g = \beta_0 + \alpha_0 \, . \tag{10}$$

Also, the NMO velocity values should be corrected to those values that would be obtained on a horizontal measurement surface without near-surface velocity gradient. In the global coordinate system, the following definition holds for the NMO velocity:

$$t_{hyp}^2(h_g, m_g - x_0 = 0) = t_0^2 + \frac{4h_g^2}{v_{NMO}^2} \text{ , with} \tag{11a}$$

$$(v_{NMO}^g)^2 = \frac{2v_0 \cos^2\alpha_0}{t_0\left(K_{NIP}\cos^2\beta_0 - K_0\cos\beta_0 - v_0\,E_0\right)} \, . \tag{11b}$$

Similarly, on a fictitious planar and horizontal measurement surface through X_0 with $E_0 = 0$, the obtained NMO velocity (in global as well as in local coordinates) reads

$$v_{NMO,H}^2 = \frac{2v_0}{t_0 K_{NIP}\cos^2\beta_0^g} \, . \tag{12}$$

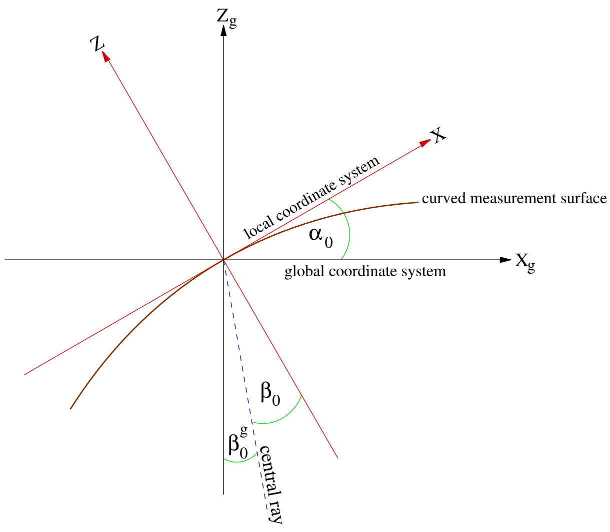

Figure 2: *The relationship between the take-off angles of the normal ray, β_0 and β_0^g, and the dip angle α_0 for a curved measurement surface. Note that β_0 is measured in the local and β_0^g in the global coordinate system. The angles are defined in the mathematical positive direction of rotation (counterclockwise). Consequently, β_0 has a negative value in the figure above.*
Please note: For this figure the origin of the global coordinate system is chosen to coincide with X_0, which is also the origin of the local coordinate system. Of course, this is, in general, not the case.

Thus, one can solve Equation (12) for K_{NIP} and insert the result into Equation (11b) to obtain the relationship between the measured NMO velocity and its corresponding value $v_{NMO,H}$ that would be measured on a fictitious horizontal surface through X_0 without near-surface velocity gradient. Doing this results in the relation

$$v_{NMO,H}^2 = \frac{2(v_{NMO}^g)^2 v_0 \, \frac{\cos^2\beta_0}{\cos^2\beta_0^g}}{(v_{NMO}^g)^2(K_0\,\cos\beta_0 t_0 + v_0 E_0 t_0) + 2v_0\cos^2\alpha_0} \, . \tag{13}$$

Applying these transformations leads to attribute sections, which represent those values of the respective attribute that refer to a fictitious horizontal measurement surface without near-surface velocity gradient. However, it has to be taken into account that, in general, the elevation of these fictitious reference surfaces is different for different central points $X_0 = (x_0, z_0)$. This means for the attribute sections $S_i(x_0, t_0)$ and also for the ZO section $S_{ZO}(x_0, t_0)$ that, in general, every x_0 is related to a different elevation z_0. The consequence is that, e.g., in case of a measurement surface with sinusoidal shape and a subsurface constituted of homogeneous layers separated by horizontal reflectors, one would find sinusoidal images of the reflectors in the ZO section. The same observation would hold for the attribute sections. To remove this undesired topography effect from the ZO section and the attribute sections, I introduce a fictitious horizontal measurement surface to which all attributes and traveltimes are related. In other words, a situation is simulated in which all central rays start and end at the same

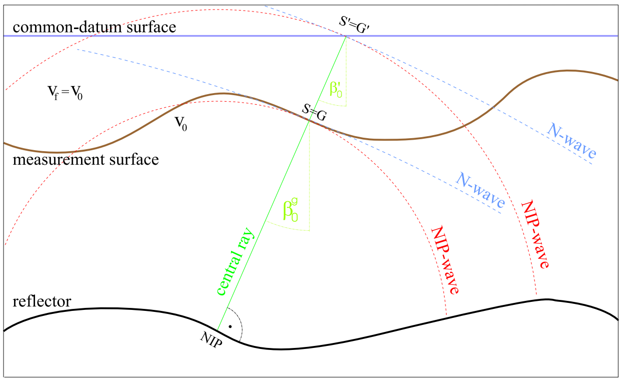

Figure 3: *To remove the influence of the acquisition surface topography from the obtained ZO and attribute sections, a situation is simulated where all central rays end on the same horizontal measurement surface, called common-datum surface. Here, this is shown for one central ray. In order to keep the figure simple, only the situation $(\nabla v)_0 = 0$ is displayed, were refraction at the measurement surface does not have to be considered, as one can choose $v_f = v_0$.*

horizonal measurement surface. Thus, one has to transfer the zero-offset traveltimes and also the attributes to those values, which would be measured on this *common-datum surface*. Such a procedure is called *redatuming*. In the following, all values that pertain to this virtual measurement surface are denoted with a prime. The key information for this procedure is the knowledge of the take-off angle β_0, which is provided by the CRS stack. If the common-datum surface is assumed to be above the actual topography, it is possible to choose an arbitrary velocity v_f for the fictitious layer between the topography and the new datum. If the near-surface velocity gradient is zero, then the most convenient choice is to set v_f equal v_0, because this avoids that the real measurement surface has to be considered as an additional reflector. For $(\nabla v)_0 \neq \mathbf{0}$ Snell's Law has to be considered to derive β_0', the fictitious take-off angle at the fictitious coincident source and receiver point X_0'. Knowing the take-off angles and the wave velocity within the fictitious layer, it is not difficult to forward propagate the N- and NIP-wave fronts upwards to the common-datum surface.

Mapping of X_0 and t_0 to the common-datum surface

To map the coincident source and receiver point X_0 of a central ray from the original measurement surface to its corresponding location X_0' at the common-datum surface, one has to transform its coordinates x_0 and z_0 to their new values x_0' and z_0'. Of course, z_0' is given by the elevation of the common-datum surface. To transfer x_0 one has to know the emergence angle of the central ray after being refracted at the measurement surface. I will denote this angle as β_0^f. Here, the well-known Snell's Law reads

$$\frac{v_0}{v_f} = \frac{\sin\beta_0}{\sin\beta_f}\,, \tag{14}$$

and solving for β_0^f leads to

$$\beta_0^f = \arcsin\left(\frac{v_f}{v_0}\sin\beta_0\right)\,. \tag{15}$$

In analogy to Equation (10), the take-off angle measured at the common-datum surface β_0' is given by

$$\beta_0' = \beta_0^f + \alpha_0\,. \tag{16}$$

Denoting the vertical distance between X_0 and the common-datum surface as Δz, simple trigonometric considerations lead to the relation between x_0 and x_0'

$$x_0' = x_0 + \Delta z \tan\beta_0'\,. \tag{17}$$

Similarly, one obtains for the new two-way traveltime of the central ray

$$t_0' = t_0 + \frac{2\Delta z}{v_f\cos\beta_0'}\,. \tag{18}$$

To avoid very long equations I have abstained here and in the following from substituting the primed values by unprimed ones using previously derived Equations.

Mapping of K_N and K_{NIP} to the common-datum surface

In order to transfer the values of the wavefield attributes K_N and K_{NIP} to those values which would be measured at the common-datum surface, one has to use the *refraction law* (see, e.g., Hubral and Krey, 1980) that gives us the curvature of the N- and NIP-wave, respectively, after passing the measurement surface. This leads to the following equation(s):

$$K_{N,NIP}^f = \frac{K_{N,NIP}v_f\cos^2\beta_0}{v_0\cos^2\beta_0^f} + \frac{K_0}{\cos^2\beta_0^f}\left(\frac{v_f}{v_o}\cos\beta_0 - \cos\beta_0^f\right)\,, \tag{19}$$

where $K_{N,NIP}^f$ are the refracted wavefront curvatures of the N- and NIP-wave, respectively, on the upper side of the measurement surface. Finally, one applies the *transmission law* (see, e.g., Hubral and Krey, 1980) to propagate the wavefronts of the N- and NIP-wave through the fictitious layer above the real measurement surface upwards to the common-datum surface. The resulting wavefront curvatures K_N' and K_{NIP}' measured at the common-datum surface are

$$\frac{1}{K_{N,NIP}'} = \left(\frac{1}{K_{N,NIP}^f} + \frac{1}{2}v_f t_f\right)\,, \tag{20}$$

with the two-way traveltime within the fictitious layer given by

$$t_f = t_0' - t_0 = \frac{2\Delta z}{v_f\cos\beta_0'}\,. \tag{21}$$

Mapping of v_{NMO} to the common-datum surface

According to Equation (11b), the NMO velocity obtained on a fictitious, planar (K_0= 0), and horizontal (α_0= 0) measurement surface through X_0 with constant near-surface velocity (E_0= 0) is given by Equation (12). Consequently, the NMO velocity as it would be measured at the common-datum surface is given by

$$v_{NMO}' = \sqrt{\frac{2v_f}{t_0' K_{NIP}'\cos^2\beta_0'}}\,. \tag{22}$$

Conclusions

Within the last years the 2-D ZO CRS stack, assuming a planar measurement surface and a constant near-surface velocity, was applied in many cases with great success. However, in any case where these conditions were not met, coarse static corrections have been unavoidable. In this abstract I have reviewed and extended a new approach, that is able to consider both, the local dip and curvature of the measurement surface and the near-surface velocity gradient. Even though there may also be cases, where the conditions demanded by this more general approach were not fulfilled, the required static corrections are much smaller. From the implementational point of view, the presented formulation of the CRS stacking operator in global coordinates provides a considerable simplification. By this means, 90% of the existing 2-D ZO CRS stack code can be reused in an efficient and convenient way. The computational cost of this more general approach is more or less the same as for the conventional 2-D ZO CRS stack, as the search for the wavefield attributes, which is the most time consuming part, remains the same. The three wavefield attributes, which are determined as a byproduct of the CRS stack procedure, are the basis of the powerful redatuming formalism presented in this abstract. The importance of this additional step is evident in view of further processing and final interpretation. Nevertheless, redatuming is only one of the various valuable applications of the CRS wavefield attributes.

Acknowledgments

I would like to thank the sponsors of the Wave Inversion Technology (WIT) Consortium for their support.

References

Bergler, S. (2001). Common-Reflection-Surface stack for common offset - theory and application. Master's thesis, Karlsruhe University.

Bortfeld, R. (1989). Geometrical ray theory: Rays and traveltimes in seismic systems (second-order approximations of the traveltime). *Geophysics*, 48(3):1342–349.

Chira, P., Tygel, M., Zhang, Y., and Hubral, P. (2001). Analytic CRS stack formula for a 2D curved measurement surface and finite-offset reflections. *Journal of Seismic Exploration*, 10(1-3):245–262.

de Bazelaire, E. (1988). Normal moveout revisited - inhomogeneous media and curved interfaces. *Geophysics*, 53(2):143–157.

de Bazelaire, E. and Viallix, J. R. (1994). Normal moveout in focus. In *Extended Abstracts, 54th Mtg. Eur. Assoc. Expl. Geophys.*, pages 174–175.

Duveneck, E. (2003). Determination of velocity models from data-derived wavefront attributes. In *Extended Abstracts, EAGE 65th Conf. and Tech. Exhib.*, Session: D027.

Gelchinsky, B., Berkovitch, A., and Keydar, S. (1997). *Multifocusing homeomorphic imaging: Parts I und II*. Special Course on Homeomorphic Imaging. Wave Inversion Technology Consortium, Geophysical Institute, Karlsruhe University.

Gurevich, B., Keydar, S., and Landa, E. (2001). Multifocusing imaging over an irregular topography. *Geophysics*, 67(2):639–643.

Höcht, G. (1998). Common-Reflection-Surface stack. Master's thesis, Karlsruhe University.

Höcht, G. (2002). *Traveltime approximations for 2D and 3D media and kinematic wavefield attributes*. PhD thesis, Karlsruhe University. http://www.ubka.uni-karlsruhe.de/indexer-vvv/2002/physik/3.

Hubral, P. (1983). Computing true amplitude reflections in a laterally inhomogeneous earth. *Geophysics*, 48(8):1051–1062.

Hubral, P., editor (1999). *Special Issue on Macro-Model Independent Seismic Reflection Imaging*, volume 42(3,4) of *Journal of Applied Geophysics*, Amsterdam. Elsevier.

Hubral, P. and Krey, T. (1980). *Interval velocities from seismic reflection traveltime measurements*. Soc. Expl. Geophys.

Mann, J. (2002). *Extentions and applications of the Common-Reflection-Surface stack method*. PhD thesis, Karlsruhe University. Logos Verlag, Berlin.

Müller, T. (1999). *The Common-Reflection-Surface stack method - seismic imaging without explicit knowledge of the velocity model*. PhD thesis, Karlsruhe University. Der andere Verlag, Bad Iburg.

Zhang, Y., Bergler, S., and Hubral, P. (2001). Common-Reflection-Surface (CRS) stack for common offset. *Geophysical Prospecting*, 49(6):709–718.

Zhang, Y., Höcht, G., and Hubral, P. (2002). 2D and 3D ZO CRS stack for a complex top-surface topography. In *Extended Abstracts, 64th EAGE Conference*, Session: P166.